CNS-resident progenitors direct the vascularization of neighboring tissues

Ryota L. Matsuoka[a,1], Andrea Rossi[a], Oliver A. Stone[a], and Didier Y. R. Stainier[a,1]

[a]Department of Developmental Genetics, Max Planck Institute for Heart and Lung Research, Bad Nauheim 61231, Germany

Edited by Igor B. Dawid, The Eunice Kennedy Shriver National Institute of Child Health and Human Development National Institutes of Health, Bethesda, MD, and approved August 8, 2017 (received for review November 27, 2016)

Organ growth requires the coordinated invasion and expansion of blood vessel networks directed by tissue-resident cells and morphogenetic cues. A striking example of this intercellular communication is the vascularization of the central nervous system (CNS), which is driven by neuronal progenitors, including neuroepithelial cells and radial glia. Although the importance of neuronal progenitors in vascular development within the CNS is well recognized, how these progenitors regulate the vasculature outside the CNS remains largely unknown. Here we show that CNS-resident radial glia direct the vascularization of neighboring tissues during development. We find that genetic ablation of radial glia in zebrafish larvae leads to a complete loss of the bilateral vertebral arteries (VTAs) that extend along the ventrolateral sides of the spinal cord. Importantly, VTA formation is not affected by ablation of other CNS cell types, and radial glia ablation also compromises the subsequent formation of the peri-neural vascular plexus (PNVP), a vascular network that surrounds the CNS and is critical for CNS angiogenesis. Mechanistically, we find that radial glia control these processes via Vegfab/Vegfr2 signaling: *vegfab* is expressed by radial glia, and genetic or pharmacological inhibition of Vegfab/Vegfr2 signaling blocks the formation of the VTAs and subsequently of the PNVP. Moreover, mosaic overexpression of Vegfab in radial glia is sufficient to partially rescue the VTA formation defect in *vegfab* mutants. Thus, our findings identify a critical function for CNS-resident progenitors in the regulation of vascularization outside the CNS, serving as a paradigm for cross-tissue coordination of vascular morphogenesis and growth.

angiogenesis | spinal cord | zebrafish | radial glia | Vegf signaling

The vascular system functions in the delivery of oxygen, nutrients, and hormones, thereby providing fundamental support for tissue growth, homeostasis, and function. During development, the vascularization of the central nervous system (CNS) initiates by angiogenic sprouting from the peri-neural vascular plexus (PNVP) into neural tissues (1–4). This angiogenic sprouting event is directed primarily by morphogenetic cues that derive from CNS-resident cells. Neuronal progenitors, including neuroepithelial cells and radial glia, secrete factors, including Wnts and Vegfs, which promote the ingression of blood vessels into neural tissues (5–9). The metabolic state of neurons (10, 11) as well as signals from specialized CNS glia (12, 13) also play instructive roles in vascular patterning in the developing CNS. In contrast to these recent advances in our understanding of CNS vascularization, however, the cellular and molecular bases of vascular assembly around the CNS remain poorly understood.

We have recently begun to investigate the role of different CNS cell types in vascular development around the CNS by optimizing genetic ablation conditions for these cell types in zebrafish (14). This ablation method uses the bacterial enzyme Nitroreductase (NTR), which triggers cell apoptosis upon administration of a prodrug substrate, metronidazole (Mtz) (15, 16). Using cell type-specific promoters to drive NTR expression, different CNS cell types can be ablated in a spatially and temporally controlled manner. By using this ablation technology, we previously identified a requirement for radial glia during embryonic stages in limiting the oversprouting of the vasculature around the spinal cord, thereby ensuring the formation of a precisely patterned network (14). Prior work has suggested that the developing neural tube provides signals to recruit the endothelial cells (ECs) that form the PNVP (4, 17). However, the angiogenic events leading to PNVP formation as well as the cellular and molecular bases of this process remain largely unknown. By using unique attributes of the zebrafish model, we address these questions and identify a specific CNS cell type that is required to drive the formation of the PNVP around the spinal cord.

Results

Specific Cell-Type Ablation Using Genetic and Pharmacological Tools. The developing zebrafish CNS is known to comprise different glial and neuronal cell types. The major cell types include radial glia neuronal progenitors, neurons, oligodendrocytes, and microglia. Unlike in the mammalian CNS, radial glia neuronal progenitors persist in many regions of the adult zebrafish CNS (18, 19), and to date, there is no clear evidence for bona fide astrocytes in the developing zebrafish spinal cord at the stages we analyzed in this study [3–30 days post fertilization (dpf)].

To investigate whether and how these CNS cell types control vascular development around the CNS, we ablated each of these cell types during development. To ablate radial glia, we used the *TgBAC(gfap:gal4ff)* line, in which Gal4ff is driven by the *gfap* regulatory elements contained in a BAC (14, 19). By crossing the *TgBAC(gfap:gal4ff)* line with the *Tg(UAS-E1b:Eco.NfsB-mCherry)* line, which contains an NTR-mCherry fusion cassette under the control of the upstream activator sequence (UAS), we generated *TgBAC(gfap:gal4ff);Tg(UAS-E1b:Eco.NfsB-mCherry)*

Significance

The formation of the vascular network surrounding the central nervous system (CNS) is important for its subsequent vascularization. Previous work has suggested that the developing neural tube provides signals to recruit the endothelial cells that form the peri-neural vascular plexus (PNVP), a vascular network that surrounds the CNS. Here, we identify a critical role for CNS-resident progenitors in directing multistep angiogenic processes required for PNVP formation. Genetic ablation of CNS-resident progenitors in zebrafish affects the formation of the vascular network in tissues adjacent to the spinal cord. Genetic inactivation of Vegfab/Vegfr2 signaling phenocopies these vascular defects, and CNS-resident progenitors serve as a source of Vegfab. Mosaic overexpression of Vegfab in these progenitors induces ectopic blood vessels directed toward their endfeet.

Author contributions: R.L.M. and D.Y.R.S. designed research; R.L.M. performed research; A.R. and O.A.S. contributed new reagents/analytic tools; R.L.M. and D.Y.R.S. analyzed data; and R.L.M. and D.Y.R.S. wrote the paper.

The authors declare no conflict of interest.

This article is a PNAS Direct Submission.

[1]To whom correspondence may be addressed. Email: Ryota.Matsuoka@mpi-bn.mpg.de or didier.stainier@mpi-bn.mpg.de.

This article contains supporting information online at www.pnas.org/lookup/suppl/doi:10.1073/pnas.1619300114/-/DCSupplemental.

fish, abbreviated *Tg(gfap:NTR)*. To ablate neurons, we used *Tg(elavl3:gal4-vp16);Tg(UAS-E1b:Eco.NfsB-mCherry)* fish, abbreviated *Tg(elavl3:NTR)*. To ablate oligodendrocytes, we used *Tg(mbpa:gal4-vp16);Tg(UAS-E1b:Eco.NfsB-mCherry)* fish, abbreviated *Tg(mbpa:NTR)*. For microglia depletion, we used *irf8* mutants, which were shown to lack microglia throughout development (20). Moreover, we treated embryos with a Sonic Hedgehog signaling inhibitor, cyclopamine, from 34 to 52 hours post fertilization (hpf), which was previously shown to result in a dramatic loss of spinal cord oligodendrocytes and their precursors (21).

We first confirmed that the *Tg(gfap:NTR)* line we used specifically labels GFAP-positive radial glia at the larval stage when we induced cell ablation (Fig. S1 *A–B″*), and we tested whether these transgenic (Tg) lines, as well as the cyclopamine treatment, could ablate the target cells effectively (Figs. S1 *C–J″* and S2 *A–D*). We further observed that ablation of radial glia and neurons is specific for each of these cell types (Fig. S2 *G–K″*).

Genetic Ablation of CNS Radial Glia, but Not of Other CNS Cell Types, Leads to a Complete Loss of the Vertebral Arteries. To determine whether and how these CNS cell types regulate vascular development, each Tg line was crossed with the EC reporter Tg line, *Tg(kdrl:EGFP)*. We treated larvae with 2 mM Mtz starting from 78 hpf and assessed vascular development at 178 hpf (Fig. 1*A*). Interestingly, we observed that radial glia-ablated fish exhibited largely comparable patterns of the trunk vasculature to controls. However, we found that the vertebral arteries (VTAs), which develop along the ventrolateral sides of the spinal cord, were completely absent in 178 hpf radial glia-ablated fish (Fig. 1 *B* and *C*). This phenotype is fully penetrant and was observed in all of the radial glia-ablated animals analyzed (Fig. 1*F* and Table S1; $n = 20$). VTAs were present in all of the 178 hpf DMSO or 2 mM Mtz-treated control fish examined (Fig. 1 *B* and *F*; $n = 20$). Intriguingly, neuronal ablation did not lead to VTA formation defects (Fig. 1 *D–F*; $n = 20$). Importantly, fish depleted for oligodendrocytes, oligodendrocyte precursor cells, or microglia also did not exhibit this defect (Fig. S2 *A–F*), suggesting a specific role for radial glia in regulating VTA formation.

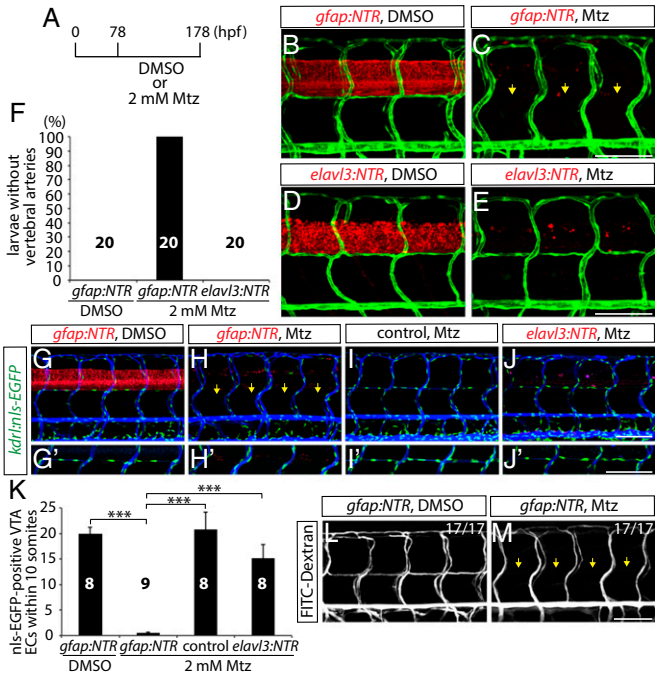

Fig. 1. Genetic ablation of CNS radial glia in early larval stages leads to a complete loss of the VTAs. (*A*) Experimental time course for *B–E*, *G–J*, *L*, and *M*. (*B–E*) 178 hpf *Tg(gfap:NTR)* (*B* and *C*) and *Tg(elavl3:NTR)* (*D* and *E*) trunk vasculature visualized by *Tg(kdrl:*EGFP*)* expression after treatment with DMSO (*B* and *D*) or Mtz (*C* and *E*). Genetic ablation of radial glia, but not of neurons, leads to the loss of the VTAs (yellow arrows, *C*). (*F*) Percentage of larvae without VTAs, as judged by *Tg(kdrl:*EGFP*)* expression (10 somites examined per animal). (*G–J*) 178 hpf *Tg(gfap:NTR)* (*G* and *H*), control (*I*), and *Tg(elavl3:NTR)* (*J*) animals carrying the *kdrl:nls-EGFP* transgene, which were injected with Q-dot 655 nanocrystals after treatment with DMSO (*G*) or Mtz (*H–J*). Radial glia-ablated fish lack ECs in the position of the VTAs (yellow arrows, *H*). High-magnification images of ECs in the position of the VTAs are shown in *G′–J′*. (*K*) Quantification of nls-EGFP$^+$ EC number in the position of the VTAs within 10 somites per animal. Values represent means ± SEM, ***$P < 0.001$. (*L* and *M*) 178 hpf *Tg(gfap:NTR)* trunk vasculature visualized by FITC-dextran microangiography after treatment with DMSO (*L*) or Mtz (*M*). Radial glia ablation leads to a loss of lumenized VTAs (yellow arrows, *M*). (Scale bar, 100 μm.)

Next, we quantified the number of ECs that form the VTAs using the *Tg(kdrl:NLS-EGFP)* reporter line after radial glia ablation. Consistent with the observations with *Tg(kdrl:*EGFP*)* expression, the number of ECs in the position of VTAs dramatically decreased in radial glia-ablated fish compared with control or neuron-ablated fish (Fig. 1 *G–K* and Table S1; $n = 8–9$ for each group). We also found the absence of lumenized VTAs by FITC-dextran microangiography (Fig. 1 *L* and *M*; $n = 17$). In control fish, FITC-dextran nanocrystals that were injected into the common cardinal vein circulated and labeled the trunk vasculature, including the VTAs (Fig. 1*L*). However, VTAs were not labeled by FITC-dextran nanocrystals in radial glia-ablated fish (Fig. 1*M*). These results indicate that radial glia ablation leads to a loss of the ECs that form the VTAs, resulting in the absence of these vessels. Thus, radial glia act as positive regulators of VTA formation.

VTAs Are Important for Subsequent Vascularization Around and Within the Spinal Cord. We next examined a developmental time course of VTA formation and observed that VTAs are formed later than other major trunk vessels such as the intersegmental vessels (ISVs) (Fig. 2 *A–D*). The cells that form the VTAs begin sprouting from the ISVs between 76 and 102 hpf, and VTA formation appears to be mostly complete by around 7–8 dpf (Fig. 2 *A–D* and Movie S1). We also observed that VTAs show strong expression of the *Tg(-0.8flt1:*tdTomato*)* arterial marker, but not the *Tg(lyve1:*DsRed*)* venous and lymphatic marker, at 8 dpf (Fig. S3 *A–B″*), suggesting that these vessels are of arterial identity (Fig. S3*C*; 132 VTAs quantified, $n = 12$ fish). Importantly, we found that cellular processes extending from radial glia, marked by *TgBAC(gfap:*Gfap-EGFP*)* expression, lie in close proximity to VTAs throughout development (Fig. 2 *B–F″*).

At later developmental stages (11 dpf), we found that VTAs, as well as ISVs, initiate a secondary angiogenic program that vascularizes the peri-neural tissue between the dorsal ISVs and subsequently forms the PNVP, a vascular network that surrounds the spinal cord (Fig. 2 *G* and *H*, Fig. S3 *D* and *E*, and Movie S2). By 15 dpf, the sprouting vessels that derive from VTAs and ISVs further extend and connect with neighboring VTAs and ISVs (Fig. 2*I*). Importantly, we found that VTAs serve as critical scaffolds for PNVP formation (Fig. 2*J* and Fig. S3*F*). At around 17–18 dpf, when the PNVP becomes established, EC invasion into the spinal cord begins in its dorsolateral sides (Movie S3). These spinal cord-invading ECs originate from the PNVP (Fig. 2 *K* and *L* and Movie S3), and vessel growth is maintained through later stages (Fig. 2 *M–O* and Movies S4 and S5). These observations show that the VTAs serve as important vascular scaffolds for the subsequent vascularization in and around the spinal cord.

Vegfab/Vegfr2 Signaling Is Necessary for VTA Formation. We next investigated how radial glia positively regulate VTA formation in vivo. To determine which angiogenic stimuli regulate VTA formation, we treated *Tg(kdrl:ras-mcherry)* fish with small molecules that inhibit distinct angiogenic signaling pathways. Specifically, we treated the larvae with the following compounds from 80 to 152 hpf: 2 μM sunitinib, a broad receptor tyrosine

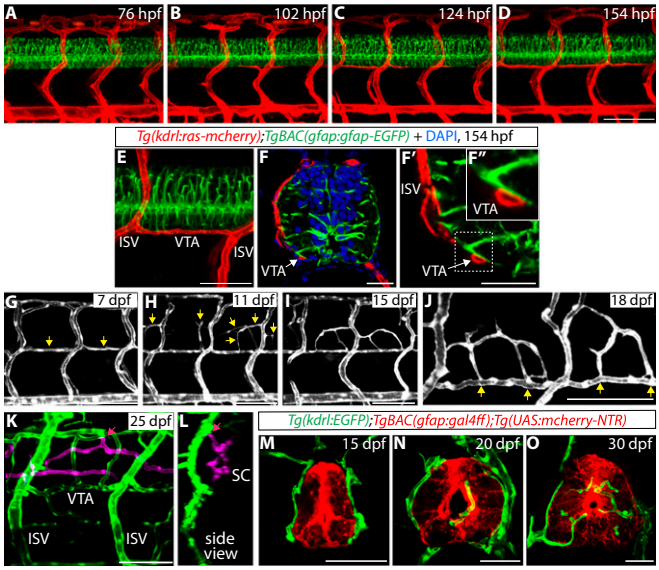

Fig. 2. VTAs serve as critical scaffolds for subsequent vascularization around and within the spinal cord. (*A–D*) *TgBAC(gfap:gfap-EGFP);Tg(kdrl:ras-mcherry)* trunks at 76 (*A*), 102 (*B*), 124 (*C*), and 154 (*D*) hpf show a developmental time course of VTA formation. (*E* and *F–F″*) A 154 hpf *TgBAC(gfap:gfap-EGFP);Tg(kdrl:ras-mcherry)* trunk (*E*) and its sections counterstained with DAPI (*F–F″*). Radial glia endfeet and VTAs are physically adjacent (white arrows). High-magnification image of the region inside the dashed line (*F′*) is shown in *F″*. (*G–I*) *Tg(kdrl:EGFP)* trunk vasculature at different developmental stages. At 7 dpf, most VTAs are formed (*G*, yellow arrows). At 11 dpf, sprouting vessels emerge between dorsal ISVs (*H*, yellow arrows), and these vessels have established connections with neighboring VTAs or ISVs by 15 dpf (*I*). (*J*) High-magnification image of *Tg(kdrl:EGFP)* trunk vasculature at 18 dpf. Vessels around the spinal cord are connected to VTAs (yellow arrows). (*K* and *L*) *z*-stack projection images of 25 dpf *Tg(kdrl:EGFP)* trunk vasculature. Blood vessels inside the spinal cord are shown in magenta. Pink arrows point to the sites where angiogenic sprouting into the spinal cord takes place. It mostly occurs from the dorsolateral sides of the PNVP. (*M–O*) *Tg(gfap:NTR);Tg(kdrl:EGFP)* trunk sections at different developmental stages. At 15 dpf, blood vessels are not observed inside the spinal cord (*M*). Blood vessel invasion into the spinal cord is observed by 20 dpf (*N*). Increased number and density of spinal cord vessels are observed at 30 dpf (*O*). (Scale bars, 100 μm in *D* and *G–K*, 50 μm in *E* and *M–O*, and 20 μm in *F* and *F′*.)

kinase inhibitor; 2.5 μM SKLB1002, a selective Vegfr2 inhibitor; 10 μM LY294002, a selective PI3 kinase inhibitor; 5 μM DMHI, a selective Bmp receptor inhibitor; and 3 μM PD158780, a selective ErbB receptor tyrosine kinase inhibitor. Among the chemicals tested, DMHI or PD158780 treatment did not affect VTA formation (Fig. 3*I*; $n = 16$ for each treatment group), suggesting that VTA formation is not regulated by BmpR or ErbB signaling. In contrast, VTA formation was dramatically inhibited in larvae treated with sunitinib, SKLB1002, or LY294002 (Fig. 3 *A–D*; quantification shown in Fig. 3*I* and Table S1; $n = 16$), suggesting that the Vegfr2 signaling pathway regulates this process. To investigate Vegfr2 effector pathways involved in VTA formation, we tested the following chemicals: 50 μM SB203580, a p38-MAPK inhibitor; 100 μM PF573228, a FAK inhibitor; 500 nM U73122, a PLC inhibitor; 10 μM SL327, a MEK1/2 inhibitor; 100 μM SU6656, a SRC kinase inhibitor; 50 μM SH-6, an AKT inhibitor; and 50 nM wortmannin, a PI3 kinase inhibitor. Interestingly, only when larvae were treated with SH-6 or wortmannin was VTA formation significantly inhibited (Fig. S4; $n = 12$). Similar results were obtained by treating the larvae with another PI3K inhibitor, LY294002 (Fig. 3*D*). Altogether, these data indicate that the PI3K-AKT pathway is a major Vegfr2 effector pathway required for VTA formation.

We further tested these observations by using genetic tools that block Vegfr2 or Vegfr3 signaling in a temporally controlled manner. To this aim, we used two Tg lines: the *Tg(hsp70l:sflt1)* line, which upon heat shock overexpresses a soluble form of Vegfr1 (sFlt1), a decoy receptor for Vegfa, Vegfb, and PIGF (22), and the *Tg(hsp70l:sflt4)* line, which upon heat shock overexpresses a soluble form of Vegfr3 (sFlt4), a decoy receptor for Vegfc and Vegfd (22). We crossed the *Tg(hsp70l:sflt1)* and *Tg(hsp70l:sflt4)* lines with the *Tg(kdrl:NLS-EGFP)* line and heat shocked larvae every 12 h starting at 74 hpf until 7 dpf. We found that overexpression of sFlt1, but not sFlt4, significantly reduced the number of ECs that form VTAs (Fig. 3 *E–H′*; quantification shown in Fig. 3*J* and Table S1; $n = 10$). Altogether, these pharmacological and genetic data are consistent with a role for Vegfr2 signaling in VTA formation.

To identify the Vegfr2 ligand(s) regulating VTA formation, we analyzed different Vegfr2 ligand mutants, including *vegfaa*^{bns1}, *vegfab*^{bns92}, and *vegfc*^{hu6410} (23) mutant animals. We recently generated and characterized *vegfaa*^{bns1} mutants that exhibit severe vasculogenesis and angiogenesis defects, leading to a lack of blood circulation, pericardial edema, and early larval death (24, 25). In addition, we generated a *vegfab*^{bns92} mutant allele by targeted genome editing using the CRISPR/Cas9 system (25). In this mutant, the cysteine residues critical for the knot motif are

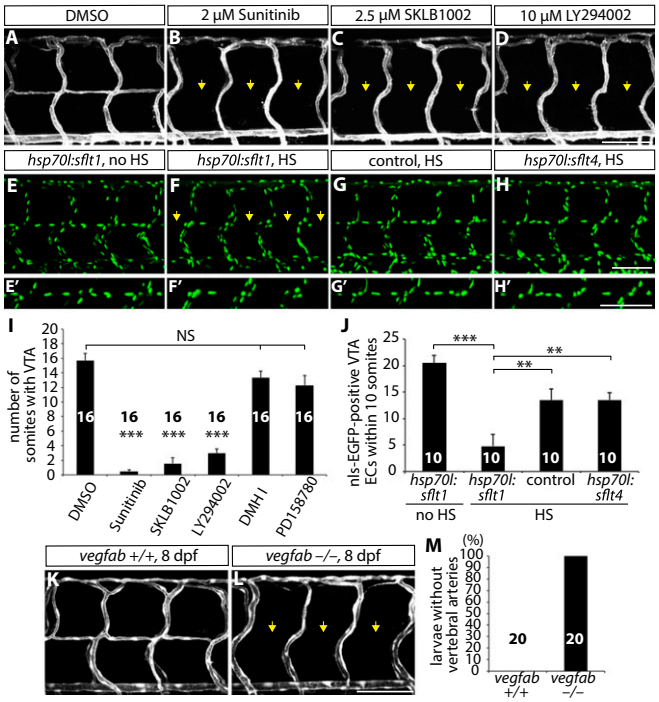

Fig. 3. Vegfab/Vegfr2 signaling is required for VTA formation. (*A–D*) 152 hpf *Tg(kdrl:ras-mcherry)* trunk vasculature after treatment with DMSO (*A*), Sunitinib (*B*), SKLB1002 (*C*), or LY294002 (*D*) starting at 80 hpf. Sunitinib, SKLB1002, and LY294002 treatments significantly inhibit VTA formation (yellow arrows). (*E–H*) 178 hpf *Tg(hsp70l:sflt1)* (*E* and *F*), control (*G*), and *Tg(hsp70l:sflt4)* (*H*) trunk ECs visualized by *Tg(kdrl:*nls-EGFP) expression. Larvae were subjected to no heat shock (HS) (*E*) or multiple heat shocks (*F–H*). High-magnification images of ECs in the position of the VTAs are shown in *E′–H′*. Overexpression of sFlt-1 leads to a significantly reduced number of ECs in the position of the VTAs (yellow arrows, *F*). (*I*) Quantification of the average number of somites with VTAs for the experiments *A–D* (20 somites examined per animal). (*J*) Quantification of nls-EGFP^{+} EC number in the position of the VTAs within 10 somites per animal for the experiments *E–H*. (*K* and *L*) 8 dpf *TgBAC(etv2:EGFP) vegfab*$^{+/+}$ (*K*) and *vegfab*$^{-/-}$ (*L*) trunk vasculature. All *vegfab*$^{-/-}$ larvae examined ($n = 20$) lacked VTAs (yellow arrows). (*M*) Percentage of larvae without VTAs, as judged by *TgBAC(etv2:*EGFP) expression. Values represent means ± SEM (*I* and *J*), $^{**}P < 0.01$ and $^{***}P < 0.001$. (Scale bar, 100 μm.)

DEVELOPMENTAL BIOLOGY

lost, thus affecting Vegf dimerization and function (25) (Fig. S5*A*). Therefore, *vegfab*^{bns92} is likely to be a severe or even a null allele (25). By carefully analyzing VTA formation in *vegfaa*^{bns1}, *vegfab*^{bns92}, and *vegfc*^{hu6410} mutant animals, we found that the *vegfab*^{bns92} mutants show a fully penetrant loss of VTA phenotype, as observed in radial glia-ablated fish (Fig. 3 *K–M* and Table S1; $n = 20$ for *vegfab*$^{+/+}$ and *vegfab*$^{-/-}$). We observed that VTAs never fully form in *vegfab*^{bns92} mutants examined up to 15 dpf (Fig. 3*L*). In contrast, *vegfc*^{hu6410} or *vegfaa*^{bns1} (a *hsp70l:vegfaa*$_{165}$ transgene was used to rescue the early vasculogenesis and angiogenesis phenotypes of *vegfaa*^{bns1} mutants by heat shock-induced overexpression of Vegfaa$_{165}$ at 10 and 24 hpf) mutant animals do not exhibit a VTA formation defect [Fig. S5 *B* and *C*; $n = 11$ for *Tg(hsp70l:vegfaa*$_{165}$*) vegfaa*$^{-/-}$ and $n = 10$ for *vegfc*$^{-/-}$ larvae]. We also documented the absence of lumenized VTAs in *vegfab*^{bns92} mutants by FITC-dextran microangiography (Fig. S5 *D* and *E*; $n = 10$). Thus, these analyses reveal that Vegfab signaling through Vegfr2 is essential for VTA formation.

We next tested whether the depletion of sFlt1, a Vegf decoy receptor, rescues the lack of VTAs observed in *vegfab*^{bns92} mutants since a loss of sFlt1 causes ectopic vascular sprouting from dorsal ISVs (14, 26) and leads to increased Vegf bioavailability (22). To this aim, we analyzed *flt1*^{bns29};*vegfab*^{bns92} double mutants and observed that VTA formation was not rescued by increasing the bioavailability of other Vegfs (Fig. S6 *A–D* and *F*), providing further evidence that Vegfab is specifically required for VTA formation. We also observed that the ectopic ISV sprouting present in *flt1*^{bns29} mutants was also present in *flt1*^{bns29};*vegfab*^{bns92} double mutants (Fig. S6 *A–E*), suggesting that this ectopic sprouting process is regulated by Vegfs other than Vegfab. Furthermore, we found similar ISV oversprouting and/or a lack of VTA phenotypes when we performed radial glia ablation in *Tg(gfap:NTR)* animals by Mtz treatments starting at developmental stages earlier than 78 hpf (Figs. S6 *G–M* and S7), supporting a role for radial glia in the regulation of these two distinct processes. These phenotypes were not observed in larvae in which neurons were ablated by Mtz treatment starting at different developmental stages (14) (Fig. 1*E* and Fig. S6 *N–P*).

***vegfab* Is Expressed by Radial Glia, and Radial Glia Ablation Leads to Greatly Reduced *vegfab* Expression Within the Spinal Cord.** To examine the expression pattern of *vegfab*, we performed whole-mount in situ hybridization at 80 hpf when VTA formation takes place. We found that *vegfab* is strongly expressed in the head, spinal cord, and endoderm-derived organs at 80 hpf (Fig. 4 *A–A″*) and that *vegfab* expression in the brain and spinal cord, but not in endoderm-derived organs, is markedly reduced in radial glia-ablated fish (Fig. 4 *A–B″*). These data indicate that radial glia serve as a source of *vegfab* and/or regulate its expression within the spinal cord to promote VTA formation. To investigate whether *vegfab* is expressed in radial glia, we generated a BAC construct containing the *vegfab* regulatory elements and driving expression of Gal4ff and injected it into *Tg(gfap:GFP);Tg(14XUAS:mCherry-MA)* one-cell stage embryos (Fig. 4*C*). We found that mCherry-positive spinal cord cells were colabeled by *Tg(gfap:*GFP*)* expression at the stages when VTA formation occurs (3–7 dpf) as well as at later stages including 10 and 13 dpf (Fig. 4 *D–D″*). These data indicate that *vegfab* is expressed by spinal cord radial glia. Taken together, these findings suggest that radial glia serve as a source of Vegfab for VTA formation, which is dependent on Vegfab/Vegfr2 signaling.

Radial Glia Ablation at Later Stages Leads to Compromised PNVP Formation. We next asked whether PNVP formation was regulated by radial glia. To this aim, we treated *Tg(gfap:NTR)* larvae with DMSO or 2 mM Mtz from 9 to 11 dpf. Interestingly, we found that DMSO-treated larvae exhibited robust sprouting of vessels between the dorsal ISVs at 11 dpf (Fig. 4*E*; $n = 14$); however, radial glia-ablated fish showed a dramatically reduced number of these sprouting vessels (Fig. 4*F*; $n = 15$). In contrast, we did not observe a significant reduction in the number of these

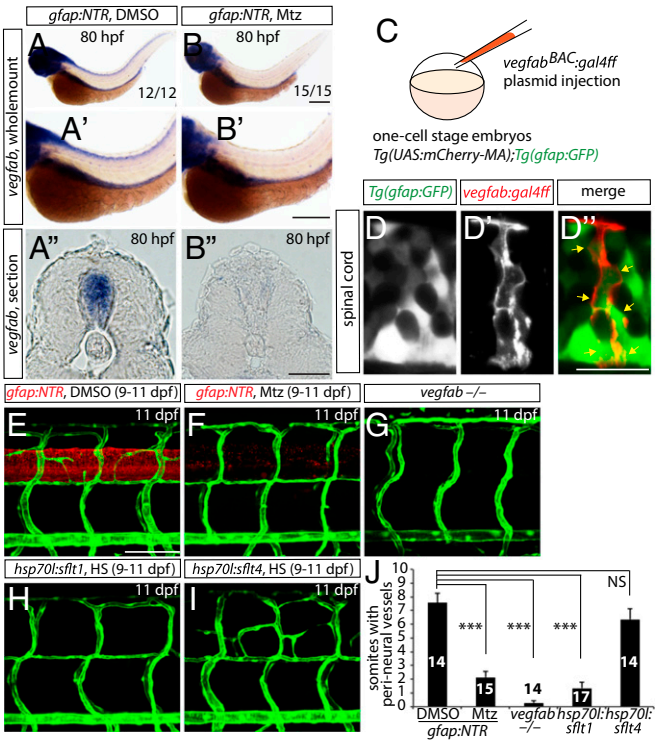

Fig. 4. *vegfab* is expressed by radial glia, and radial glia-ablated fish as well as *vegfab* mutants fail to develop a PNVP around the spinal cord. (*A* and *B*) Whole-mount in situ hybridization for *vegfab* expression in 80 hpf *Tg(gfap:NTR)* larvae treated with DMSO (*A*) or Mtz (*B*) starting at 30 hpf. High-magnification images of the trunk regions and their cryosections are shown in (*A′* and *B′*) and (*A″* and *B″*), respectively. Mtz-treated fish show decreased *vegfab* transcripts in the spinal cord compared with DMSO-treated fish. (*C*) Schematic diagram of the plasmid injection experiments (*D–D″*). (*D–D″*) 105 hpf *Tg(UAS:mcherry-MA);Tg(gfap:GFP)* trunk of fish injected with the *vegfab* BAC plasmid that drives Gal4ff. Injection of the plasmid drives mCherry expression in cells within the spinal cord (*D′*), which are also positive for *Tg(gfap:*GFP*)* expression (*D*). Most mCherry^{+} cells are also GFP^{+} (*D″*, yellow arrows). (*E–I*) 11 dpf *Tg(gfap:NTR)* trunk vasculature after treatment with DMSO (*E*) or Mtz (*F*) starting at 9 dpf; 11 dpf *TgBAC(etv2:EGFP) vegfab*$^{-/-}$ (*G*), *Tg(kdrl:EGFP);Tg(hsp70l:sflt1)* (*H*), and *Tg(kdrl:EGFP);Tg(hsp70l:sflt4)* (*I*) trunk vasculature after heat shocks (*H* and *I*). DMSO-treated control fish display vessels that emerge between dorsal ISVs around the spinal cord; however, vessel formation is severely impaired in radial glia-ablated larvae as well as in *vegfab*$^{-/-}$ animals. Overexpression of sFlt1 also blocked PNVP formation. (*J*) Quantification of the average number of somites with peri-neural blood vessels (10 somites examined per animal). Values represent means ± SEM, ***$P < 0.001$. (Scale bars, 200 μm in *B–B″*, 100 μm in *E*, and 20 μm in *D″*.)

sprouting vessels in larvae in which neurons, oligodendrocytes, or microglia were ablated (Fig. S8 *A–E*; $n = 16–20$). These findings suggest that radial glia also direct PNVP formation. Mechanistically, we observed that *vegfab*^{bns92} mutants exhibited both VTA and PNVP formation defects (Fig. 4*G*; $n = 14$) and that genetic inhibition of Vegfr2, but not Vegfr3, signaling after VTA formation by overexpression of sFlt1 or sFlt4, respectively, blocked PNVP formation (Fig. 4 *H–J* and Table S1; $n = 14–17$). Taken together, these findings suggest that radial glia control the formation of both VTAs and PNVP in the mesodermal tissues around the spinal cord through Vegfab/Vegfr2 signaling and before the vascularization of the spinal cord.

Mosaic Overexpression of Vegfab in Radial Glia Is Sufficient to Partially Rescue the Loss of VTAs in *vegfab* Mutants and Induce Ectopic Blood Vessels Directed Toward Their Endfeet. To test whether forced Vegfab expression in spinal cord radial glia was sufficient to rescue the lack of VTAs observed in *vegfab*^{bns92} mutants, we generated

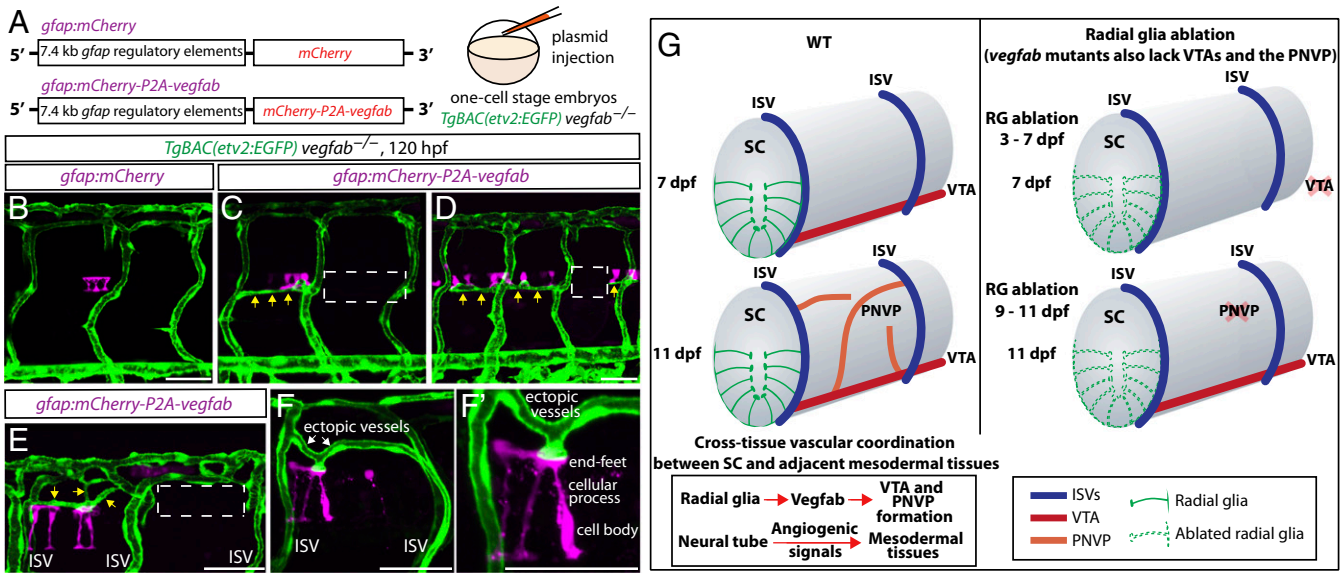

Fig. 5. Mosaic overexpression of Vegfab in radial glia is sufficient to partially rescue the loss of VTAs in *vegfab* mutants and induce ectopic blood vessels directed toward their endfeet. (*A*) Schematic diagram of the *gfap:mCherry* and *gfap:mCherry-P2A-vegfab* plasmid injection experiments (*B–F′*). (*B–F′*) 120 hpf *TgBAC(etv2:EGFP)* trunks of *vegfab*$^{-/-}$ fish injected with the *gfap:mCherry* (*B*) or *gfap:mCherry-P2A-vegfab* (*C–F′*) plasmid. Partial recovery of VTAs was observed in the *vegfab*$^{-/-}$ fish injected with the *gfap:mCherry-P2A-vegfab* plasmid (yellow arrows, *C* and *D*), while VTAs were absent in the *vegfab*$^{-/-}$ fish injected with the *gfap:mCherry* plasmid (*B*). As observed in the regions inside the dashed lines (*C* and *D*), VTAs were absent in the somites where mCherry^{+} radial glia were not present in close proximity and/or sufficient numbers. Ectopic blood vessel sprouting toward mCherry^{+} radial glia overexpressing Vegfab (yellow arrows, *E*) was not observed in somites lacking mCherry^{+} radial glia (e.g., the region inside the dashed white line in *E*). Ectopic vessels (white arrows) were directed toward the endfeet of mCherry^{+} radial glia overexpressing Vegfab (*F* and *F′*). (Scale bar, 50 μm.) (*G*) Schematic diagrams showing radial glia regulation of angiogenesis around the developing spinal cord. During development, radial glia endfeet lie in close proximity to the forming VTAs. Radial glia ablation in early larval stages leads to the loss of the VTAs. Radial glia ablation at later stages impairs PNVP formation. *vegfab* mutants phenocopy the vascular defects observed in radial glia-ablated larvae. Thus, radial glia act as positive angiogenic regulators in mesodermal tissues around the spinal cord, which in turn allows spinal cord vascularization. Vessels are shown only on one side of the spinal cord. RG, radial glia; SC, spinal cord.

plasmids that drive the expression of mCherry or mCherry-P2A-Vegfab under the control of the *gfap* promoter (27) (Fig. 5*A*). Injection of these plasmids into one-cell stage embryos led to mosaic overexpression of these transgenes in spinal cord radial glia as confirmed by mCherry expression in *Tg(gfap:*GFP*)*-positive radial glia (Fig. S8 *F–F″*). By injecting these plasmids into one-cell stage *vegfab*^{bns92} mutant embryos, we observed that mosaic overexpression of mCherry-P2A-Vegfab, but not mCherry, in radial glia was sufficient to rescue the absence of VTAs in *vegfab*^{bns92} mutants, leading to a partial recovery of VTAs (Fig. 5 *B–D*). Intriguingly, we also observed that Vegfab overexpression in radial glia led to the appearance of ectopic blood vessels in tissues adjacent to the spinal cord and that these ectopic vessels were directed preferentially toward their endfeet (Fig. 5 *E–F′*). Collectively, our data indicate that Vegfab derived from radial glia is presented to extraneural vessels through their endfeet.

Discussion

In this work, we identify a previously unappreciated role for CNS-resident progenitors in driving angiogenesis in tissues adjacent to the CNS (Fig. 5*G*). Specifically, we show that CNS radial glia ablation impairs the formation of the VTAs and PNVP, that Vegfab/Vegfr2 signaling mediates these angiogenic processes, that radial glia express *vegfab* at the stages when these vascular events occur, and that overexpression of Vegfab in radial glia is sufficient to rescue the loss of VTAs in *vegfab*^{bns92} mutants. Importantly, we find that these radial glia-directed angiogenic events are closely linked to spinal cord vascularization and provide high-resolution 3D reconstructions of the vasculature during these processes (Movies S1–S5). These findings will significantly advance our knowledge of the angiogenic steps leading to spinal cord vascularization.

How are the vascular networks around the CNS established during development? Previous work using neural tube and presomitic mesoderm cocultures has suggested that the developing neural tube provides VEGF signals to recruit the ECs that form the PNVP (4). Adding to this prior finding, we showed in vivo that ablation of radial glia, but not of other differentiated CNS cell types, leads to a defect in angiogenesis in tissues adjacent to the spinal cord, a process that is dependent on Vegfab/Vegfr2 signaling. These findings provide clear evidence that CNS-resident progenitors direct angiogenic processes not only within the CNS as previously described (5–9) but also in tissues outside the CNS, significantly adding to our understanding of the function of CNS progenitors during development. Also, these observations serve as an important example for a mechanism by which tissue vascularization is coordinated by interactions between neighboring tissues during development.

How are the angiogenesis events around the spinal cord spatiotemporally regulated? We found that angiogenesis in the mesodermal tissues around the spinal cord proceeds in a tightly controlled manner. After ISVs are formed, VTAs develop by angiogenic sprouting from ISVs. After VTA formation is complete, peri-neural vessels emerge from both ISVs and VTAs to form the PNVP around the spinal cord by connecting with these vessels. When these angiogenic steps are complete, spinal cord vascularization begins by angiogenic sprouting from the established PNVP into the spinal cord. Our data show that radial glia initiate this multistep angiogenic process at least in part via Vegfab. Given the observation that forced Vegfab expression in radial glia induced ectopic blood vessels directed toward their endfeet (Fig. 5 *E–F′*), we speculate that Vegfab secreted from radial glia may be presented to extraneural vessels through their endfeet to guide VTA and PNVP formation. VTA formation was not rescued by other Vegfs, such as Vegfaa, in the absence of Vegfab (Fig. S6 *D* and *F*), possibly because Vegfaa and Vegfab appear to have different properties (25). The Vegf decoy receptor sFlt1 was recently shown to limit the oversprouting of the dorsal ISVs around the spinal cord during early larval stages

(3–6 dpf) (14, 26). In *sflt1* mutants, sprouting vessels emerge from the ISVs around the spinal cord by 6 dpf (14, 26), in contrast to WT fish where this sprouting occurs at much later stages (10–15 dpf), indicating that sFlt1 is, at least in part, involved in the spatiotemporal regulation of these angiogenic processes.

We recently reported that radial glia ablation initiated at 30 hpf leads to selective oversprouting of venous ISVs around the spinal cord, showing a role for radial glia as negative angiogenic regulators (14). In contrast, here we show that inducing radial glia ablation at later stages leads to impaired formation of VTAs, indicating a role for radial glia as positive angiogenic regulators. These two contrasting observations could indicate that (*i*) spinal cord radial glia control angiogenesis differentially at distinct developmental stages, (*ii*) different ECs (i.e., venous vs. arterial) respond differently to the loss of radial glia, and/or (*iii*) distinct populations of radial glia extend their endfeet in close proximity to ISVs or VTAs and affect these vessels differently. When *Tg(gfap:NTR)* animals were treated with Mtz starting at 30 hpf, we occasionally observed vessels emerging in positions where VTAs form (Figs. S6*H* and S7); however, these vessels did not appear when we replaced the Mtz with freshly prepared Mtz at 78 hpf (Fig. S6*L*), suggesting that a more complete ablation of radial glia starting at 30 hpf abrogates VTA formation, an interpretation different from the one which might be drawn from looking at Fig. 2*C* in our previous report (14). Notably and consistent with our previous findings (14), radial glia ablation induced under this stronger Mtz treatment led to ectopic vISV sprouting (Fig. S6*L*).

Altogether, our identification of a critical role for CNS-resident progenitors in regulating angiogenesis in adjacent mesodermal tissues will advance our understanding of the mechanisms governing vascular network formation, in particular how tissue vascularization between adjacent organs is coordinated during development.

Materials and Methods

Detailed materials and methods are available in *SI Materials and Methods*.

Zebrafish. Procedures involving animals were approved by the veterinary department of the Regional Board of Darmstadt.

Mtz Treatment. Mtz treatment was performed as described previously (14).

Heat Shock Treatments. Heat shock treatments were performed as previously described (14).

Statistical Analysis. Statistical differences for mean values among multiple groups were determined using a one-way analysis of variance (ANOVA) followed by Tukey's multiple comparison test.

ACKNOWLEDGMENTS. We thank Hae-Chul Park for fish lines, Petra Neeb and Rebecca Lee for technical assistance, and Michele Marass and Arica Beisaw for comments on the manuscript. This work was supported by funding from the Damon Runyon Cancer Research Foundation (DRG#2104-12), Human Frontier Science Program (LT001023/2012-L), Japan Society for the Promotion of Science, Excellence Cluster Cardio-Pulmonary System, and German Centre for Cardiovascular Research (to R.L.M.) and NIH Grant HL54737, the Packard Foundation, and the Max Planck Society (to D.Y.R.S.).

1. Feeney JF, Jr, Watterson RL (1946) The development of the vascular pattern within the walls of the central nervous system of the chick embryo. *J Morphol* 78:231–303.
2. Strong LH (1964) The early embryonic pattern of internal vascularization of the mammalian cerebral cortex. *J Comp Neurol* 123:121–138.
3. Kurz H, Gärtner T, Eggli PS, Christ B (1996) First blood vessels in the avian neural tube are formed by a combination of dorsal angioblast immigration and ventral sprouting of endothelial cells. *Dev Biol* 173:133–147.
4. Hogan KA, Ambler CA, Chapman DL, Bautch VL (2004) The neural tube patterns vessels developmentally using the VEGF signaling pathway. *Development* 131: 1503–1513.
5. Haigh JJ, et al. (2003) Cortical and retinal defects caused by dosage-dependent reductions in VEGF-A paracrine signaling. *Dev Biol* 262:225–241.
6. Raab S, et al. (2004) Impaired brain angiogenesis and neuronal apoptosis induced by conditional homozygous inactivation of vascular endothelial growth factor. *Thromb Haemost* 91:595–605.
7. Stenman JM, et al. (2008) Canonical Wnt signaling regulates organ-specific assembly and differentiation of CNS vasculature. *Science* 322:1247–1250.
8. Daneman R, et al. (2009) Wnt/beta-catenin signaling is required for CNS, but not non-CNS, angiogenesis. *Proc Natl Acad Sci USA* 106:641–646.
9. Liebner S, et al. (2008) Wnt/beta-catenin signaling controls development of the blood-brain barrier. *J Cell Biol* 183:409–417.
10. Lacoste B, et al. (2014) Sensory-related neural activity regulates the structure of vascular networks in the cerebral cortex. *Neuron* 83:1117–1130.
11. Whiteus C, Freitas C, Grutzendler J (2014) Perturbed neural activity disrupts cerebral angiogenesis during a postnatal critical period. *Nature* 505:407–411.
12. Ye X, et al. (2009) Norrin, frizzled-4, and Lrp5 signaling in endothelial cells controls a genetic program for retinal vascularization. *Cell* 139:285–298.
13. Wang Y, et al. (2012) Norrin/Frizzled4 signaling in retinal vascular development and blood brain barrier plasticity. *Cell* 151:1332–1344.
14. Matsuoka RL, et al. (2016) Radial glia regulate vascular patterning around the developing spinal cord. *eLife* 5:e20253.
15. Curado S, et al. (2007) Conditional targeted cell ablation in zebrafish: A new tool for regeneration studies. *Dev Dyn* 236:1025–1035.
16. Pisharath H, Rhee JM, Swanson MA, Leach SD, Parsons MJ (2007) Targeted ablation of beta cells in the embryonic zebrafish pancreas using E. coli nitroreductase. *Mech Dev* 124:218–229.
17. Chapman DL, Papaioannou VE (1998) Three neural tubes in mouse embryos with mutations in the T-box gene Tbx6. *Nature* 391:695–697.
18. Than-Trong E, Bally-Cuif L (2015) Radial glia and neural progenitors in the adult zebrafish central nervous system. *Glia* 63:1406–1428.
19. Lam CS, März M, Strähle U (2009) gfap and nestin reporter lines reveal characteristics of neural progenitors in the adult zebrafish brain. *Dev Dyn* 238:475–486.
20. Shiau CE, Kaufman Z, Meireles AM, Talbot WS (2015) Differential requirement for irf8 in formation of embryonic and adult macrophages in zebrafish. *PLoS One* 10: e0117513.
21. Schebesta M, Serluca FC (2009) olig1 expression identifies developing oligodendrocytes in zebrafish and requires hedgehog and notch signaling. *Dev Dyn* 238:887–898.
22. Ruiz de Almodovar C, Lambrechts D, Mazzone M, Carmeliet P (2009) Role and therapeutic potential of VEGF in the nervous system. *Physiol Rev* 89:607–648.
23. Helker CSM, et al. (2013) The zebrafish common cardinal veins develop by a novel mechanism: Lumen ensheathment. *Development* 140:2776–2786.
24. Koenig AL, et al. (2016) Vegfa signaling promotes zebrafish intestinal vasculature development through endothelial cell migration from the posterior cardinal vein. *Dev Biol* 411:115–127.
25. Rossi A, et al. (2016) Regulation of Vegf signaling by natural and synthetic ligands. *Blood* 128:2359–2366.
26. Wild R, et al. (2017) Neuronal sFlt1 and Vegfaa determine venous sprouting and spinal cord vascularization. *Nat Commun* 8:13991.
27. Bernardos RL, Raymond PA (2006) GFAP transgenic zebrafish. *Gene Expr Patterns* 6: 1007–1013.
28. Jin SW, Beis D, Mitchell T, Chen JN, Stainier DY (2005) Cellular and molecular analyses of vascular tube and lumen formation in zebrafish. *Development* 132:5199–5209.
29. Blum Y, et al. (2008) Complex cell rearrangements during intersegmental vessel sprouting and vessel fusion in the zebrafish embryo. *Dev Biol* 316:312–322.
30. Chi NC, et al. (2008) Foxn4 directly regulates tbx2b expression and atrioventricular canal formation. *Genes Dev* 22:734–739.
31. Proulx K, Lu A, Sumanas S (2010) Cranial vasculature in zebrafish forms by angioblast cluster-derived angiogenesis. *Dev Biol* 348:34–46.
32. Bussmann J, et al. (2010) Arteries provide essential guidance cues for lymphatic endothelial cells in the zebrafish trunk. *Development* 137:2653–2657.
33. Okuda KS, et al. (2012) lyve1 expression reveals novel lymphatic vessels and new mechanisms for lymphatic vessel development in zebrafish. *Development* 139: 2381–2391.
34. Stevenson TJ, et al. (2012) Hypoxia disruption of vertebrate CNS pathfinding through ephrinB2 is rescued by magnesium. *PLoS Genet* 8:e1002638.
35. Park HC, et al. (2000) Analysis of upstream elements in the HuC promoter leads to the establishment of transgenic zebrafish with fluorescent neurons. *Dev Biol* 227: 279–293.
36. Chung AY, et al. (2013) Generation of demyelination models by targeted ablation of oligodendrocytes in the zebrafish CNS. *Mol Cells* 36:82–87.
37. Davison JM, et al. (2007) Transactivation from Gal4-VP16 transgenic insertions for tissue-specific cell labeling and ablation in zebrafish. *Dev Biol* 304:811–824.
38. Heap LA, Goh CC, Kassahn KS, Scott EK (2013) Cerebellar output in zebrafish: An analysis of spatial patterns and topography in eurydendroid cell projections. *Front Neural Circuits* 7:53.
39. Carney TJ, et al. (2006) A direct role for Sox10 in specification of neural crest-derived sensory neurons. *Development* 133:4619–4630.
40. Matsuoka RL, et al. (2011) Transmembrane semaphorin signalling controls laminar stratification in the mammalian retina. *Nature* 470:259–263.
41. Thisse C, Thisse B (2008) High-resolution in situ hybridization to whole-mount zebrafish embryos. *Nat Protoc* 3:59–69.
42. Bussmann J, Schulte-Merker S (2011) Rapid BAC selection for tol2-mediated transgenesis in zebrafish. *Development* 138:4327–4332.